MPPT Perturb - Observe Algorithm with Fuzzy Logic for a Dual Active Bridge-Series Resonant Converter

James Rolando Arredondo-Mamani[1](✉), Mario Gaston Borja-Borja[2], Marco Antonio Quispe-Barra[1], Jorge Apaza-Cruz[1], Gabino Vidangos-Ponce[1], Russel Lozada-Vilca[1], and Oliver Amadeo Vilca-Huayta[1]

[1] Universidad Nacional del Altiplano, Puno, Peru
{jarredondo,marcoquispe,jlapaza,gvidangos,rlozada,ovilca}@unap.edu.pe
[2] Universidad Nacional de Ingeniería, Lima, Peru
mborja@uni.edu.pe

Abstract. This article analyzes a solar photovoltaic system composed of a Series Resonant Active Dual Bridge DC-DC Converter and its control blocks. These converters are particularly attractive for renewable energy applications due to their high switching frequency with low switching losses. The converter analysis consists of an equivalent circuit using the Fourier series from that obtaining the control parameters. The classic MPPT Perturb-Observe algorithm is also designed and analyzed to add the Fuzzy Logic algorithm and shorten the search time for the maximum power point and reduce the oscillation around the maximum power point, which is produced by the Disturb-Observe algorithm once that point is found. Finally, the results of the simulations performed with PSIM software for a 500 W solar panel prototype are presented. The results of the classic Perturb-Observe algorithm are compared with the Perturb-Observe modified algorithm with fuzzy logic, giving a better performance than the classic one.

Keywords: DAB-SR · MPPT · Fuzzy logic · Photovoltaic system

1 Introduction

One of the fundamental parts of the PV system is the electronic power converter that allows it to generate the appropriate voltages and currents for the feeding of the loads and the extraction of the maximum power from the PV. Between the panel and the converter, there are control blocks, which ensure stable power. Electronic power converters have progressed effectively in the industry and can therefore be considered a mature and proven technology. Given the advancement of technology, these converters have been changing and modifying their structure. These power converters have broad applications in renewable energy sources, such as wind power [1] and solar photovoltaic power [2]. Among the most commonly used DC-DC converters on PV systems are the Boost converters [3], the Buck converter [4], and a combination of these structures. In [5], a

© The Author(s), under exclusive license to Springer Nature Switzerland AG 2022
Y. Iano et al. (Eds.): BTSym 2021, SIST 295, pp. 642–651, 2022.
https://doi.org/10.1007/978-3-031-08545-1_63

detailed review of several converter topologies based on the Boost and Buck converters employed to achieve the desired voltage level at the grid output is presented. The authors discuss these converters and their characteristics in terms of hardware complexity, costs, and efficiency, among others. However, in this type of converter, the efficiency depends on the switching since, as the frequency of the switches increases, the energy losses also increase. In addition, in the case of voltage boosters, there is a limited voltage gain [4]. On the other hand, another converter topology presents a high energy conversion efficiency because it decreases switching losses. These are resonant converters. Figure 1 shows a Dual Active Bridge-Series Resonant (DAB-SR) Converter. The DC input voltage is connected to the full active bridge whose keys lead and block quickly depending on the switching frequency to produce the AC voltage at high frequency to the LC circuit. The LC circuit is the resonance tank, whose behavior is a bandpass filter used to reduce losses in the converter [6]. The high-frequency transformer allows it to operate with galvanic isolation, adapting to different voltage levels. The voltage at the output can be higher or lower than the input, which is an advantage over those converters mentioned above. This converter makes it possible to take advantage of the transformer's leakage inductance as an energy transfer element and reduce the converter's size [7].

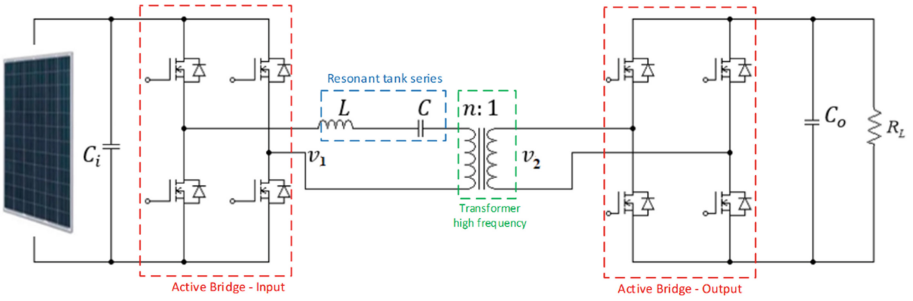

Fig. 1. Dual active bridge–series resonant converter.

The PV panel has different operating points. This will depend on the load or converter connected to the panel and on the climatic conditions such as irradiation and temperature; For this reason, to take advantage of the power available in the PV panel effectively, the converter must keep track of the maximum power point. For this purpose, a control block is necessary to perform the function of a Maximum Power Point Tracker (MPPT). The MPPT ensures that the PV panel operates at its maximum voltage and maximum current available from the panel at any given time. To find the MPPT, the functionality is achieved through various algorithms, widely studied in the literature [8, 9], which are implemented in the electronic converter.

One of the most popular algorithms is the Perturb and Observe (P&O) method [10] due to its easy implementation in the electronic converter. However, the P&O algorithm has the drawback that the size of the steps to reach the maximum power causes the calculated power to oscillate around the maximum. If the steps are small, the oscillation is less, but the time to find the maximum power is greater, but if the steps are large, the

algorithm needs less time to reach the maximum power, but the oscillation is greater. Due to this problem, in the present work, the step sizes are varied using fuzzy logic.

2 Analysis of the Photovoltaic System DAB-SR

The photovoltaic system consists of the following components, as shown in Fig. 2: Photovoltaic panel, which has an available power according to the load. The MPPT control block senses the current and voltage of the PV panel to extract the maximum available power; this goes to a PI controller, which sends a reference current signal that goes to another control block that controls the switching of the converter bridges.

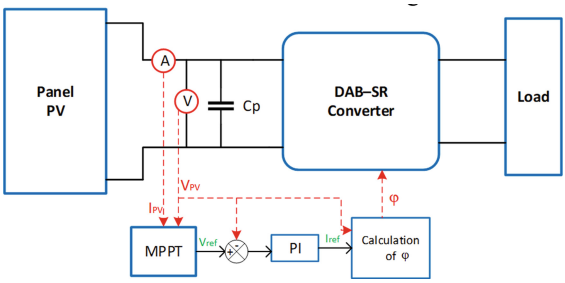

Fig. 2. Proposed photovoltaic system.

2.1 DAB-SR Converter

Figure 1 shows the DAB-SR converter circuit, connected to a PV panel and a DC voltage source. Active bridges are operated with a cyclic ratio of 50% to produce symmetrical alternating voltages (v1 and v2, respectively). Each other, the active bridges are performed with an offset angle φ, as shown in Fig. 3, where it is considered positive if the voltage v2 is delayed with respect to v1. The isolation transformer has a transformation n ratio.

The converter operates at a constant switching frequency f_s, slightly higher than the resonant frequency of the LC tank, f_r. In this way, the impedance has inductive characteristics, allowing it to control the power through the angle φ. The LC-type tank impedance is dimensioned to offer high attenuation outside the switching frequency. In this way, the circulating current can be approximated by the fundamental component with a sinusoidal format. In this way, the quantitative energy transfer analysis can be carried out considering only the fundamental components (sinusoidal) of current and voltage in the resonant tank. From Fig. 3, the expressions of v1 and v2, (1) and (2) respectively are obtained.

$$v_1 = V_i \sum_{n=1}^{\infty} \frac{4}{\pi} \frac{\sin((2n-1)\omega_s t)}{2n-1} \tag{1}$$

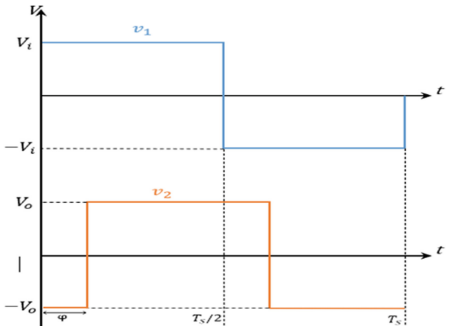

Fig. 3. Voltage waveforms in complete bridges.

$$v_2 = V_o \sum_{n=1}^{\infty} \frac{4}{\pi} \frac{\sin((2n-1)(\omega_s t - \phi))}{2n-1} \tag{2}$$

By taking only the fundamental components of the voltages v1 and v2, since the resonant tank filters the other components, the following expression can be obtained.

$$i_L = -\frac{4}{\pi} \frac{V_{in}\cos(\omega_s t) - nV_o\cos(\omega_s t - \phi)}{Z\left(F - \frac{1}{F}\right)} \tag{3}$$

Where:
$Z = \sqrt{\frac{L}{C}}$: Characteristic impedance of the tank circuit
$F = \frac{\omega_s}{\omega_r}$: Frequency ratio
$\omega_s = 2\pi f_s$: Switching frequency
$\omega_r = \frac{1}{\sqrt{LC}}$: Tank circuit resonant frequency
The average input current can be determined by (4) where the switching function of the active input bridge, m, defined in (5) [2] has been introduced:

$$I_i = \frac{1}{2\pi} \int_0^{2\pi} i_L m d\omega_s t \tag{4}$$

$$m = \frac{1}{2}\text{sgn}(\cos((\omega_s - \omega_r)t)) - \frac{1}{2}\text{sgn}(\cos((\omega_s + \omega_r)t)) \tag{5}$$

From the above expressions, (6) is obtained for the average value of the input current.

$$I_i = \frac{8n}{\pi^2 Z\left(F - \frac{1}{F}\right)} V_o \sin(\phi) \tag{6}$$

Equation (6) shows that the average input current I_i depends only on the φ gap that exists between the two bridges since the values such as the output voltage V_o, the ratio n, and the other values shown in (3) are constant. Therefore, by varying φ, the current flow is controlled. On the other hand, if you consider zero losses in the DAB-SR converter circuit, you can consider the input power as the output power. By doing this, the output current I_o depends only on V_i and the phase φ.

2.2 PV Panel

The parameters that characterize a PV panel are: the short circuit current I_{SC}, the open-circuit voltage V_{OC}, the maximum power point current IMPP, and the maximum power point voltage V_{MPP}; these characteristics are mentioned in the datasheet and vary according to the radiation and temperature of the panel.

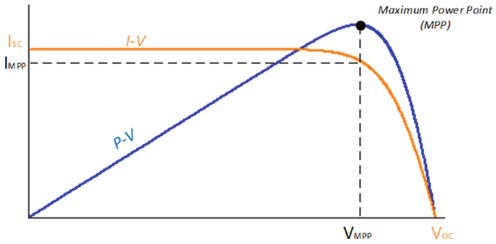

Fig. 4. Panel PV curves characteristic.

The panel presents characteristic curves I-V (current-voltage) and P–V (power–voltage) for given radiation, as shown in Fig. 4. The curves I-V and P-V are limited by I_{SC} and V_{OC}. Within this range, there are different operating points of the panel, of which a single operating point corresponds to the maximum available power. This point is defined by the V_{MPP} and I_{MPP} values of the panel, which correspond to the maximum PMPP power that the panel can deliver for given radiation. The operating point of a PV solar panel depends on the respective load; that is, the panel will have different operating points within the I_{SC} and V_{OC} range, so the power delivered by the panel will not always be the maximum. Therefore, a technique that allows tracking the MPP operating must be implemented to make the most of the panel's energy.

2.3 MPPT P&O

The P&O algorithm consists of an iterative process, in which the value of the actual power P_{act} is computed, for which the actual voltage V act and the actual current I act of the PV panel are sampled. The current power is compared to the previous power to determine whether it has increased or decreased. Once defined the variation, it is evaluated if the actual voltage is greater or less than the previous voltage. In this way, the variation to be applied in the reference voltage (V_{ref}) is determined, which is the desired voltage in the PV panel. The PI controller uses this reference voltage to set the PV panel voltage. This process leads the system to operate around the V_{MPP} voltage.

Step sizes, in this case, the $\triangle V$ determines the time to reach the MPP point, so this variation will affect the algorithm, as shown in Fig. 5. In this, you can see the advantages and disadvantages of changing the step size. Since in the P&O algorithm, the step size is constant, ideally at the start of the big step algorithm and when approaching the small step MPP to have less oscillation in the MPP, one way to achieve this is fuzzy logic.

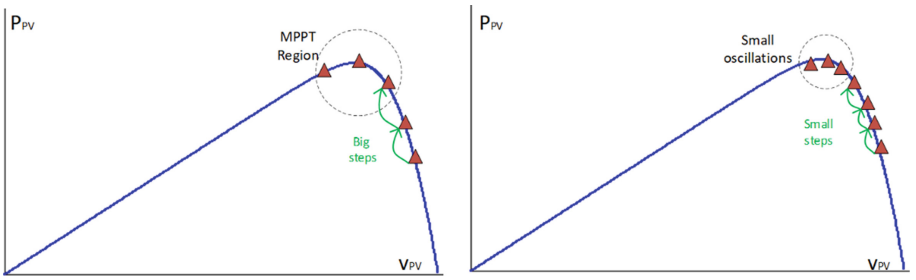

Fig. 5. MPPT P&O according to the step size.

2.4 Fuzzy Logic

Figure 6 presents the structure of the fuzzy logic algorithm (FLC). It consists of three processes: fuzzification, rules of inference, and defuzzification. In addition, the designed rules are stored in the rules table that represents the database. The process in which FLC performs the rule table-based calculation to generate the output is called fuzzy inference.

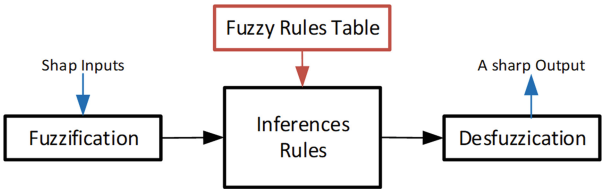

Fig. 6. Essential parts of the fuzzy logic algorithm.

3 Calculations and Analysis

3.1 DAB-SR Converter

For design purposes, the maximum voltage value that the PV panel can supply is considered the input voltage as indicated in the panel datasheet. In this case, two CORA 250 W panels are considered in order to obtain a 500 W system. A DC voltage of 311.13 V is considered at the output, which enables the subsequent connection of an inverter as an interface with the electrical grid. Other design characteristics for sizing the converter, such as the quality factor and the switching frequency, are shown in Table 1, from which the main parameters of the DAB-SR are determined.

The transformation ratio n is determined to ensure smooth switching operation ZVS. The frequency ratio, F, is 1.1 to ensure continuous driving mode. The values of fr and the different components, such as the resonant tank circuit, can be found using (6) and Table 1. The calculated values are presented in Table 2.

Table 1. Design data.

Parameter	Value
P_{PV}	250 W
P	500 W
Vi	61.3 V
Vo	311.13 V
Q	4
Fs	50 KHz

Table 2. Calculated values.

Parameter	Value
n	0.197
fr	45454.54 Hz
C	0.1436 uF
L	85.32 uH
φ	0.8689 rad

3.2 MPPT Algorithm

For the implementation of the algorithm, it is put as a linguistic variable the power variation. If the power change is small, it is defined as S (Fig. 7). If the power change is regular, it is defined as R, and, if the power change is significant, it is defined as L.

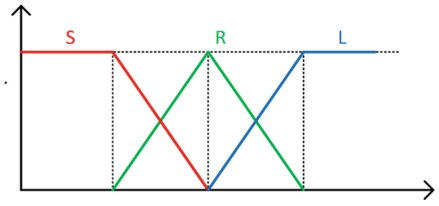

Fig. 7. Fuzzy rule.

The system's output is the step size, i.e., the voltage changes in the P&O algorithm. The outputs are defined as Small Step (SS), Normal step (NS), and Large Step (LS). The IF-THEN inference rules to determine the output state are:

```
IF VPOT=S THEN INCV=SS
IF VPOT=R THEN INCV=NS
IF VPOT=L THEN INCV=LS
```

4 Simulation and Results

The system is implemented and simulated in PSIM, and the MPPT algorithm is implemented in Block C of said software. The MPPT starts at a voltage of 55 V, from which it starts looking for the voltage that the MPP has. Figures 8 and 9 show the behavior of the classic MPPT P&O with constant passing and MPPT P&O with Fuzzy logic. In this, one could notice the remarkable improvement of the change of step using fuzzy logic. On the one hand, it finds the V_{MPP} voltage faster, approximately in 0.04 s with respect to 0.1 s, and on the other hand, it shows that it presents less oscillation around the MPP.

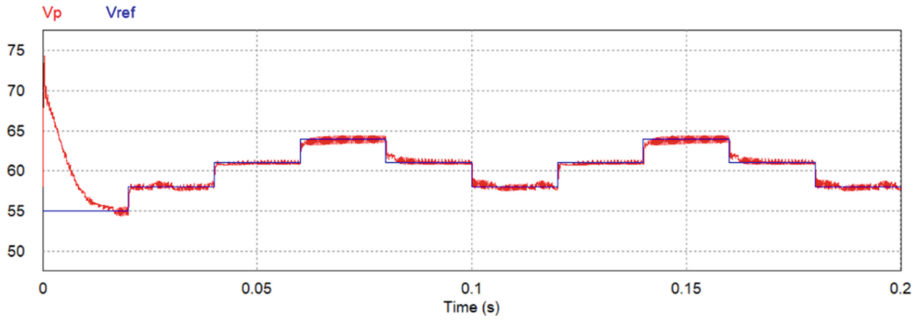

Fig. 8. Test result for voltage of the P&O algorithm.

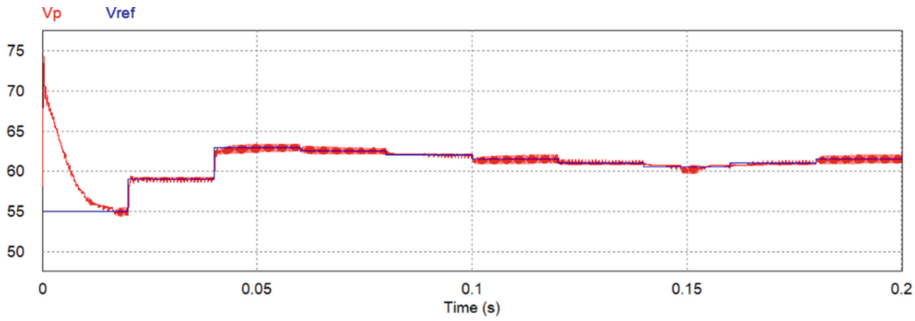

Fig. 9. Test result for voltage of the P&O with fuzzy logic algorithm.

The system has a power of 500 W. In Figs. 10 and 11, the classic MPPT P&O and the algorithm with the MPPT P&O with fuzzy logic are presented, respectively. It can be noted that the voltage has better performance than the latter algorithm.

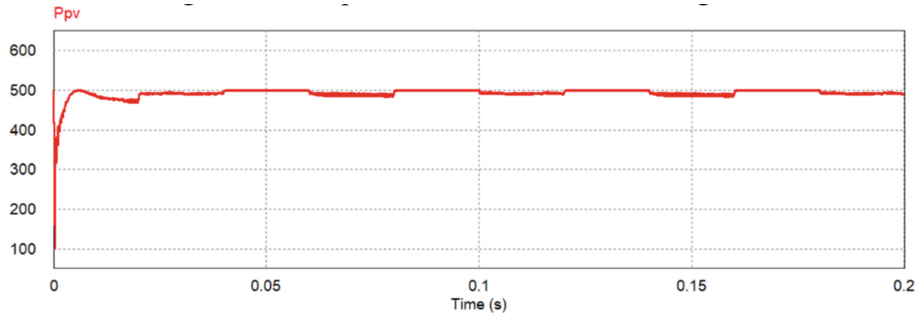

Fig. 10. Test result for the power of the P&O algorithm.

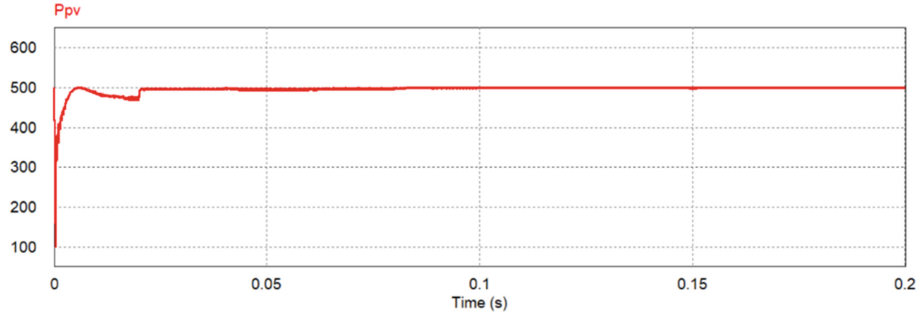

Fig. 11. Test result for the power of the P&O with fuzzy logic algorithm.

5 Conclusions

A photovoltaic system with the DAB-SR has been presented in this work using the MPPT P&O algorithm with Fuzzy Logic to change the step size. The results show that this algorithm finds the MPP quickly compared to the classic MPPT P&O algorithm. On the other hand, it shows the modulation of the bridges that show that they meet the function of the proposed design. Future work will focus on designing the fuzzy logic algorithm for this structure for partial shading conditions.

References

1. Chen, W., et al.: Analysis and comparison of medium voltage high power DC/DC converters for offshore wind energy systems. IEEE Trans. Power Electron. **28**, 2014–2023 (2014)
2. Krishnaswami, H.: Photovoltaic microinverter using single-stage isolated high-frequency link series resonant topology. In: 2011 IEEE Energy Conversion Congress and Exposition, pp. 495–500 (2011)
3. Farhat, M.: A real-time implementation of MPPT-based on P & O method (2016)
4. Venkatramanan, D., Member, S.: Dynamic modeling and analysis of buck converter based solar PV charge controller for improved MPPT performance. In: 2018 IEEE International Conference on Power Electron Drives Energy System, pp. 1–6 (2018)

5. Reshma Gopi, R., Sreejith, S.: Converter topologies in photovoltaic applications – a review. Renew. Sustain. Energy Rev. **94**, 1–14 (2018). https://doi.org/10.1016/j.rser.2018.05.047
6. Salem, M., Jusoh, A., Idris, N.R.N., Shekhar, H., Alhamrouni, I.: Resonant power converters with respect to passive storage (LC) elements and control techniques – an overview. Renew. Sustain. Energy Rev. **91**, 504–520 (2018)
7. Arredondo, J., Sal y Rosas, D.: Series-resonant DC-DC converter for solar photovoltaic non isolated applications. In: IEEE CHILEAN Conference on Electrical, Electronics Engineering, Information and Communication Technologies, Chilecon (2019)
8. Arredondo, J., Luyo, J.E.: Methods of extracting the point of maximum power (MPPT) in photovoltaic systems, an evaluation with the Entropy of Shannon. In: 2018 IEEE ANDESCON, ANDESCON 2018 - Conference Proceedings (2018)
9. Karami, N., Moubayed, N., Outbib, R.: General review and classification of different MPPT techniques. Renew. Sustain. Energy Rev. **68**, 1–18 (2017)
10. De Brito, M.A.G., Galotto, L., Sampaio, L.P., De Azevedo, M.G., Canesin, C.A.: Evaluation of the main MPPT techniques for photovoltaic applications. IEEE Trans. Ind. Electron. **60**(3), 1156–1167 (2013)